Exploring rural hospital admissions for diarrhoeal disease, malaria, pneumonia, and asthma in relation to temperature, rainfall and air pollution using wavelet transform analysis

Thandi Kapwata [a,b], Caradee Y. Wright [c,d,*], David Jean du Preez [d,e], Zamantimande Kunene [a], Angela Mathee [a,b,f,g], Takayoshi Ikeda [h], Willem Landman [d,i], Rajendra Maharaj [j], Neville Sweijd [k], Noboru Minakawa [l], Suzana Blesic [m,n]
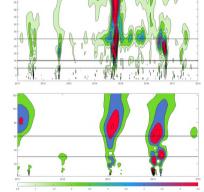
[a] Environment and Health Research Unit, South African Medical Research Council, Johannesburg, South Africa
[b] Environmental Health Department, Faculty of Health Sciences, University of Johannesburg, Johannesburg, South Africa
[c] Environment and Health Research Unit, South African Medical Research Council, Pretoria, South Africa
[d] Department of Geography, Geoinformatics and Meteorology, University of Pretoria, Pretoria, South Africa
[e] Laboratoire de l'Atmosphère et des Cyclones (UMR 8105 CNRS, Université de La Réunion, MétéoFrance), 97744 Saint-Denis de La Réunion, France
[f] School of Public Health, University of the Witwatersrand, Johannesburg 2028, South Africa
[g] Department of Environmental Health, Faculty of Health Sciences, Nelson Mandela University, Port Elizabeth, South Africa
[h] Blue Earth Security Co., Ltd., Chiyoda-ku, Tokyo, Japan
[i] International Research Institute for Climate and Society, The Earth Institute of Columbia University, New York, NY, 10964, USA
[j] Office of Malaria Research, South African Medical Research Council, Durban, South Africa
[k] Applied Centre for Climate and Earth Systems Science, National Research Foundation, Cape Town, South Africa
[l] Institute of Tropical Medicine, Nagasaki University, Nagasaki, Japan
[m] Institute for Medical Research, University of Belgrade, Belgrade, Serbia
[n] Center for Participatory Science, Belgrade, Serbia

HIGHLIGHTS

- We investigated the association between meteorology, air pollution and hospital admissions for climate-sensitive diseases
- Wavelet transform cross-correlation analysis was applied
- Increased prevalence of pneumonia related admissions follows changes in air quality after a time period of 10 to 15 days
- Increased admissions for malaria follow the co-occurrence of high temperature and rainfall after a 30-day interval
- Findings have relevance for early warning system development and climate change adaptation planning to protect human health

GRAPHICAL ABSTRACT

(Up) Local wavelet cross-correlation spectra of hospital admissions for pneumonia in comparison to $PM_{2.5}$ concentrations. (Down) Local wavelet cross-correlation spectra of hospital admissions for malaria in comparison to local rainfall data. Horizontal lines mark time delays between the onset of environmental or meteorological drive and development of diseases.

(Up) Local wavelet cross-correlation spectra of hospital admissions for pneumonia in comparison to $PM_{2.5}$ concentrations. (Down) Local wavelet cross-correlation spectra of hospital admissions for malaria in comparison to local rainfall data. Horizontal lines mark time delays between the onset of environmental or meteorological drive and development of diseases.

* Corresponding author at: South African Medical Research Council, 1 Soutpansberg Road, Pretoria 0001, South Africa.
E-mail address: Caradee.Wright@mrc.ac.za (C.Y. Wright).

ABSTRACT

Keywords:
Climate change
Environmental health
Infectious disease
Respiratory disease

Background: Climate variables impact human health and in an era of climate change, there is a pressing need to understand these relationships to best inform how such impacts are likely to change.

Objectives: This study sought to investigate time series of daily admissions from two public hospitals in Limpopo province in South Africa with climate variability and air quality.

Methods: We used wavelet transform cross-correlation analysis to monitor coincidences in changes of meteorological (temperature and rainfall) and air quality (concentrations of $PM_{2.5}$ and NO_2) variables with admissions to hospitals for gastrointestinal illnesses including diarrhoea, pneumonia-related diagnosis, malaria and asthma cases. We were interested to disentangle meteorological or environmental variables that might be associated with underlying temporal variations of disease prevalence measured through visits to hospitals.

Results: We found preconditioning of prevalence of pneumonia by changes in air quality and showed that malaria in South Africa is a multivariate event, initiated by co-occurrence of heat and rainfall. We provided new statistical estimates of time delays between the change of weather or air pollution and increase of hospital admissions for pneumonia and malaria that are addition to already known seasonal variations. We found that increase of prevalence of pneumonia follows changes in air quality after a time period of 10 to 15 days, while the increase of incidence of malaria follows the co-occurrence of high temperature and rainfall after a 30-day interval.

Discussion: Our findings have relevance for early warning system development and climate change adaptation planning to protect human health and well-being.

1. Introduction

One of the ways in which climate change influences weather patterns is by increasing the frequency, duration and intensity of extreme events including heatwaves, floods, and droughts (Seneviratne et al., 2012; Thomson et al., 2019). Climate models predict changes in heatwave attributes such as increased frequency, intensity and duration (Hales et al., 2003). These predictions show that many regions across the world can expect warmer summers and milder winters (Hales et al., 2003). Over the past five decades alone, South Africa has experienced increases of up to 1.5 °C in mean annual temperatures which is twice the global average (Ziervogel et al., 2014). Projections of future conditions based on Representative Concentration Pathway (RCP) emission scenarios demonstrate potentially large increases in flood frequency in Southeast Asia, India and eastern Africa (Hirabayashi et al., 2013). Risk of flooding is also expected to increase as global temperatures rise (Hirabayashi et al., 2013). Research has also shown that the frequency and intensity of droughts has increased in recent decades in parts of Asia and Africa and this has been attributed to changes in weather patterns caused by climate change (Ebi et al., 2003). Simulations of future climate conditions have projected increases in the occurrence of droughts over the next century for many parts of the world including most of Africa, southern Europe and the Middle East, most of the Americas, Australia, and Southeast Asia (Dai, 2011).

Associations between changes in weather patterns and air quality also exist (Jhun et al., 2015). In Canada, dry tropical weather was associated with a fourfold increase of the likelihood of an extreme pollution event due to nitrogen dioxide (NO_2), ozone (O_3), sulphur dioxide (SO_2), and particulate matter (PM) compared to moist tropical weather which resulted in a twofold increase (Vanos et al., 2015). In Greece, air pollution was higher during heatwave days than during non-heatwave days. Pollutants such as PM_{10}, NO_2 and O_3 increased by up to 38%, 29% and 12%, respectively (Papanastasiou et al., 2015).

Exposure to certain meteorological conditions and air pollution has significant impacts on human health. Consequently, the number of studies assessing the impacts of meteorological parameters and air quality on human health has grown rapidly during the last decade (Franchini and Mannucci, 2015; Kinney, 2008). Findings show that high temperatures and heatwaves result in deaths, increased hospital admissions and ambulance callouts for heat-related illnesses (see, for example, Nitschke et al., 2011; Sun et al., 2014). Extremely high rates of deaths and hospitalizations were reported during severe recent heatwave events in France, Russia, Australia and India (WMO, 2013; Fouillet et al., 2006; Akompab et al., 2013). Air pollution is another contributing factor to mortality and morbidity (Hanna et al., 2011; Vanos et al., 2014). The World Health Organization (WHO) reports that PM, O_3, NO_2 and SO_2 are the four common air pollutants that have the strongest effects on health (WHO, 2006; Bohnenstengel et al., 2015). In the United States of America, exposure to $PM_{2.5}$ was associated with 14,700 excess deaths from 1994 to 2012 (Jhun et al., 2015). It is estimated that reducing PM_{10} to the WHO annual-mean guideline of 20 μgm^{-3} would reduce attributable deaths per year in Europe by as much as 22,000 (Bohnenstengel et al., 2015).

In South Africa, associations between weather and health outcomes have been explored. Vulnerable groups such as children (Relative Risk (RR): 1.24, 95% Confidence Interval (CI): 1.15–1.34) and older adults aged 65 and older (RR: 1.13, 95% CI: 1.07–1.20) were at higher risk of mortality due to exposure to high temperatures compared to persons between 19 and 64 years of age (Scovronick et al., 2018; Wichmann, 2017). Children under 5 years of age were reportedly more vulnerable to developing diarrhoea during very dry, hot conditions as well as during periods of high rainfall because hospital admissions for diarrhoea in that age group increased significantly during these conditions (Ikeda et al., 2019). The risk of hospitalization due to cardiovascular disease on warm days increased with increasing levels of SO_2, NO_2 and PM in Cape Town (Lokotola et al., 2020).

The research that quantifies effects of air pollution, temperature and rainfall on public health are, however, lacking. Therefore, this study aimed to explain the possible relations between weather variables and air pollution on four health outcomes known to be weather and/or environment sensitive (Godsmark et al., 2019). We used wavelet transform (WT) analysis to establish possible associations between temperature, rainfall, PM and NO_2 (air pollutants for which data were available) on hospital admission symptoms relating to asthma, pneumonia, malaria, and gastrointestinal ailments obtained from admission records at two provincial hospitals in Limpopo province, South Africa.

Wavelets have been used as a data analysis tool across several scientific disciplines providing important new insights into the underlying characteristics of the signals involved (Addison, 2018). The property of WT procedure - in that it does not assume stationarity of records (Lancaster et al., 2018) - renders its applicability to research of a range of natural or human-made complex systems outputs. In this paper, we calculated wavelet power spectra (WTS), a wavelet energy density functions relatable (Perrier et al., 1995) to Fourier power spectra (PwS) to investigate global (i.e., over entire time of recording) and local (i.e., at a specific point in time) temporal behaviour of individual time series in our dataset. We furthermore used cross-wavelet transforms (CWT) comparable to cross-correlation functions (Addison,

2002) and cross-correlation coefficients (Frick et al., 2001) to discern associations between admission records in our dataset with meteorological and air quality changes, by monitoring local temporal regions of their coincidental energy (Torrence and Compo, 1998; Addison, 2018). The study findings have relevance for early warning system development and climate change adaptation planning to protect human health and well-being.

2. Methods and data

2.1. Study area

Giyani is a town in the Limpopo province of South Africa, in the far north-eastern parts of the country at approximately 525 m above sea level. We present a map of a geographic area surrounding the town in Fig. 1. The region experiences summer rainfall although summers can be extremely hot and dry. During the summer rainfall season, the area is prone to seasonal malaria which has a negative impact on public health (Gerritsen et al., 2008). This study area is vulnerable to the adverse effects of exposure to regional (from neighbouring provinces and countries) and household air pollution from the burning of wood and coal.

2.2. Hospital admission data

Handwritten, non-digitised hospital admission records for 1 January 2002 to 31 December 2017 were collected from two large public hospitals - Nkhensani Hospital and Maphutha L. Malatjie Hospital, located in

Mopani District Municipality in Limpopo province (Fig. 1). Research ethics clearance to obtain the data for analyses was granted by the South African Medical Research Council (EC005-3/2014).

Hospital records were scanned using an SV 600 overhead snap scanner, pages were saved as soft copies (i.e., PDF files) and later printed for double data entry into an electronic database using EpiData (Christiansen and Lauritsen, 2010). Each hospital admission record included patient's date of birth, patient's age, date of admission and reason for admission. The medical records included those from the children, female, and male wards only.

Gastrointestinal illnesses (GE) including diarrhoea, pneumonia-related diagnosis (hereafter called pneumonia), malaria and asthma cases were extracted from the hospital admission records database using the criteria and terms provided by South African medical doctors. Abdominal distention was not included in GE as it could be associated with a variety of medical conditions other than GE. Data were unavailable in 2006 (for reasons unknown, e.g., missing hospital admission books) for both hospitals as well as at one hospital for weeks 1–23 in 2002 and weeks 1–40 in 2007. Entries for the day of admissions were sparse for the period before 2011. Therefore, we chose the time period from the beginning of 2011 to the end of 2017 for the statistical analysis in this study, to avoid bias to the statistical function estimation that comes from artificial jumps due to the amount of missing data (Rust et al., 2008) or amplification of cyclic influence coupled with the reduction of noise due to homogenization and optimization of the raw data (Blešić et al., 2019). This provided for time series of $N = 2557$ data points for data analysis. It should be emphasized that the count for total admissions is not necessarily the total admissions at that hospital
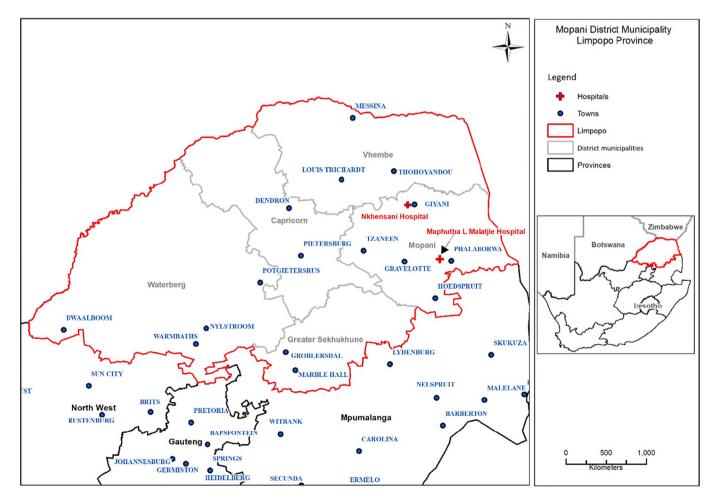

Fig. 1. Study area depicting the two hospitals in Limpopo province, South Africa.

for that day/month/year, but rather a total of the admissions that was captured by the hospital staff, collected by the researchers and entered by the data enterers.

For the purposes of detailed WT analysis – calculations of WT cross-correlation spectra - we excluded GE records for this time series includes different GE-related complications and is a complex variable that would not allow for conclusions that lead to clear dependences between the environment and 'single' disease development. We also excluded asthma records because their wavelet spectra displayed significant low-frequency cycles (annual cycle and probably higher, multi-annual cycles, please see Results below); we did not have enough data points for asthma to be able to assess effects of these cycles in a statistically meaningful way.

2.3. Temperature and rainfall data

Daily temperature data from 2011 to 2017 were obtained from the South African Weather Service. The closest operational automatic weather station was about 50 km from the area in which the two public hospitals were located. Rainfall estimate data (RFE) were obtained from RFE version 2.0 (v2.0) implemented by the National Oceanic and Atmospheric Administration's (NOAA) Climate Prediction Centre (CPC, 2001). RFE v2.0 obtains the final daily rainfall estimation by combining all satellite data using the maximum likelihood estimation method, thereafter, Global Telecommunication System (GTS) station data are used to remove bias. The daily data are then summed up to produce decadal (10-day) totals in mm for each month at a resolution of 8 km × 8 km.

2.4. Air pollution reanalysis data

Air pollution data were taken from the Copernicus Atmosphere Monitoring Service (CAMS) global reanalysis dataset. The CAMS consists of 3-dimensional atmospheric composition data, including aerosols and chemical species. It is assimilated with the European Centre for Medium range Weather Forecast's (ECMWF) Integrated Forecast System (IFS). The CAMS reanalysis data consist of 25 pressure levels with a spatial resolution of approximately 80 km at 12-hour intervals (Inness et al., 2019; ECMWF, 2021). The CAMS reanalysis dataset uses observations including O_3, NO_2, CO, methane (CH_4) and CO_2 from various satellites for input into the reanalysis data. The validation of the CAMS reanalysis data has shown that seasonal cycles of air quality parameters compare well to the observed surface data (Christophe et al., 2017). In this study, the surface daily mean values of PM with a diameter smaller than 2.5 μm ($PM_{2.5}$) and NO_2 data between 2011 and 2017 for an area over the study site were used in the WT analysis.

We provide graphs of the raw data of meteorological and air quality records that we used, with their local wavelet power spectra (please see Section 2.5 below) in the Supplementary material to this paper.

2.5. Wavelet transform analysis

Wavelet transform analysis uses localized waveform functions, called wavelets, to decompose signals akin to classical Fourier transformation (FT) decompositions (Singh et al., 2017). The advantages of the WT over FT and corresponding linked data analysis techniques lie in the method design that is based on two dimensional time (or space) and scale decomposition, which disassemble data with a basis of self-similar functions constructed by scaling (i.e. expanding by scale) and translating along the time (or space) of a specifically chosen basic wavelet function, largely referred to as 'the mother wavelet' (Torrence and Compo, 1998). This property enables investigation and visualization of dominant modes of variability (or cycles, or peaks, which are global properties of signals) and, unlike in Fourier transformations, how those modes form in time (or space, a local property of a signal) (Torrence and Compo, 1998). This is the advantage of WT that we

specifically applied in this study to inspect and compare local temporal behaviours of meteorological, environmental and hospital admissions data.

In general, the continuous wavelet transforms of any data series x_i ($i = 1...N$) is defined as:

$$W_x(a,b) = \frac{1}{\sqrt{a}} \sum_{k=1}^{N-1} x_k \psi^* \left(\frac{k-b}{a} \right), \tag{1}$$

where (*) marks the complex conjugate, while a and b are scale (dilatation) and time or space coordinate (translation) parameters that identify dilatated and translated version of the original analysing wavelet $\psi(t)$; in what follows we will mention only time as a coordinate, for we used WT to analyse time series. The general wavelet theory assumes that the whole set of wavelets $\psi(a,b) = \frac{1}{\sqrt{a}} \psi\left(\frac{k-b}{a}\right)$ is made from a single mother wavelet; to be able to properly decompose signals, mother wavelet functions are expected to meet a specific set of mathematical criteria. For further theoretical details, we refer to original articles that introduced WT analysis such as (Morlet, 1983) or (Grossmann and Morlet, 1984), or to comprehensive reviews, practical and tool guides such as (Astaf'eva, 1996), (Torrence and Compo, 1998), or (Addison, 2002).

According to the definitions given in Eq. (1), wavelet coefficients W_x (a,b) contain information about both the investigated signal and analysing wavelet function. Even if some properties of WT coefficients are independent from the choice of the analysing wavelet (Stratimirović et al., 2007), it is always important to choose the mother wavelet which is adequate for data series and the goals of the analysis. For analyses that focus on local time properties, as was the case in this study, it is better to use wavelet functions that have good localization in physical space (Frick et al., 2001). In this paper, we used Morlet wavelets as the analysing wavelet basis. Morlet wavelets (Goupillaud et al., 1984) are the most commonly used complex wavelets (Aguiar-Conraria and Soares, 2014; Addison, 2018); the analysing wavelet is a complex sinusoid in a Gaussian envelope, defined as:

$$\psi(k) = \frac{1}{\pi^{1/4}} e^{i2\pi f_0 k} e^{-k^2/2}. \tag{2}$$

In Eq. (2), f_0 represents the order, or the central frequency of the wavelet; in this study, we used Morlet wavelets of the 6th order. The choice of the order $f_0 = 6$ is determined by the mathematical criteria that in theory wavelets must meet (please see explanation of admissibility criterion in (Farge, 1992)). Morlet wavelets have to date been used to study non-stationary time series across disciplines – for analysis of records in geosciences and geophysics, in remote sensing of vegetation, in engineering, hydrology and finance, medicine, ecology and social sciences (Rhif et al., 2019). We used Morlet wavelets of the 6th order to study time series in neurosciences, economy and finance, and in climate sciences (Stratimirović et al., 2001; Stratimirović et al., 2018; Blesić et al., 2019), alone or in comparison to other wavelet groups (Stratimirović et al., 2001, 2007).

In this paper, we firstly estimated the local wavelet power spectra (LWTS), the localized contributions of the analysed time series energy at a specific time scale a and time point b, defined as:

$$E(a,b) = |W(a,b)|^2. \tag{3}$$

A plot of $E(a,b)$ is also called a scalogram and is usually presented as a colour map of intensities of WT coefficients (that is, $|W(a,b)|^2$) in real time (x-axis) and over the time scale (y-axis) plots. Such presentations enable detection of locations in time of data recording when some property developed, which manifest as changes in $|W(a,b)|^2$ values at the very onset of y-axis, and investigation of how those events contribute to dominant modes, by following their vertical (along the y-axis) variations. Each vertical line in LWTS represents a local wavelet power

spectrum for a particular time t (position at the x-axis). Finally, LWTS can be integrated (or summed, in the case of discrete datasets) over time b to produce distribution of data series energy over scale a, the global wavelet power spectrum (WTS):

$$E(a) = \frac{1}{N} \sum_{b=1}^{N-1} E(a,b). \tag{4}$$

The WTS $E(a)$ are mathematically comparable to Fourier spectra PwS (Perrier et al., 1995). In the case of records with long-range auto-correlations (the long-term persistent, or LTP data), both WTS and PwS are due to the inherent dynamics connected to such order of the power-law type (Climate Dialogue, 2014). If this is the case, both functions are linear in log-log presentations, with the same slope – power-law exponent that can be used for further characterization of such records (Blesić et al., 2019).

In this paper, we also used the cross-wavelet transform (CWT) to investigate effects of meteorological and environmental variables on hospital admission data by monitoring coincidence or similar structures between their WT energy levels. For this purpose, we used local wavelet cross-correlation spectra (LCWTS) that are for any two data series x_i and y_i ($i = 1...N$) defined (Torrence and Compo, 1998; Addison, 2002) as:
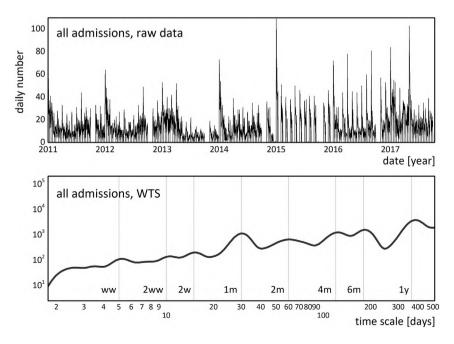
$$CE_{x,y}(a,b) = E_x^*(a,b)E_y(a,b). \tag{5}$$

The LCWTS are complex functions. In this study, we used their absolute values $|CE_{x,y}(a,b)|$ that can be visualized and inspected in the same way as wavelet scalograms LWTS. LCWTS give local covariance of different time series at each moment in time and scale and thus provide local insight into the similarity of LWTS of the two records (Aguiar-Conraria and Soares, 2014). In analogy to the global wavelet spectra, a global cross-correlation wavelet spectrum can be defined as an integral or a sum of LCWTS over time or space. Assessments of wavelet cross-correlations are usually followed by assessments of phase differences between the two records x_i and y_i. We did not calculate phase differences in this study because we assumed that the public health outcomes under investigation here tend to follow meteorological or environmental variations (Godsmark et al., 2019; Raymond et al., 2020).

To obtain statistically significant results and avoid effects of records' finite sizes on WTS statistics, we calculated WTSs between the time scales of $a = 1$ and $a = N/5$ (in our dataset, with time series length of $N = 2557$ data points (given in days), this limits investigations to approximately 17 months). We used this scale range for visualization of our results. In drawing conclusions, however, we limited ourselves to a more rigorous, maximum meaningful scale of $a_{max} = N/10$ (Koscielny-Bunde et al., 2006), which in this paper corresponds to approximately 8.5 months. To assess the significance of our results we used tests of significance for detection of cycles in WTS and CWTS functions in this study; we used the technique explained in (Torrence and Compo, 1998) against the analysed signals as LTP noise backgrounds. We provide illustration of the results of this significance testing on the wavelet spectrum of the 'all admissions' record from our dataset (please see explanation in Results below) in Supplementary material to this paper and explain our choice of the background noise. For critical assessment of some of the results related to significance testing for WT please also see Aguiar-Conraria and Soares (2014) and Rodríguez-Murillo and Filella (2020).

3. Results

Fig. 2 presents all extracted admissions records used for this study (in what follows: all admissions records or data) for the period January 2011 to December 2017 in the form of raw data (upper panel of Fig. 2) and their global wavelet spectrum (WTS, lower panel in Fig. 2). The raw admissions data show visible annual variability in all records except for year 2015 that has more missing data than other years (123 data entries for the entire year) and less daily variability (daily entries are largely for the days in the first halves of each month). In addition, records after 2015 show a slight increase in daily number of admissions in comparison to period from 2011 to 2015. Due to the amount of missing data, we were cautious when interpreting events in 2015 from our results.

The WTS spectrum of all admissions records in Fig. 2 shows cycles that are typical for human activity in the lower time scales (or high frequency) region. The cycles of five days (one working week, probably showing larger number of entries during the working week than over the weekends), 10 days (two working weeks), two weeks, and one month appear

Fig. 2. All hospital admission records (regardless of disease/illness type) for the period January 2011 to December 2017: (upper panel) raw data and (lower panel) global power spectrum. The global spectrum (WTS) presents with several cycles that are marked by the vertical light grey lines. The abbreviations in cycle annotations are the following: ww – working week, w – week, m – month and y – year.
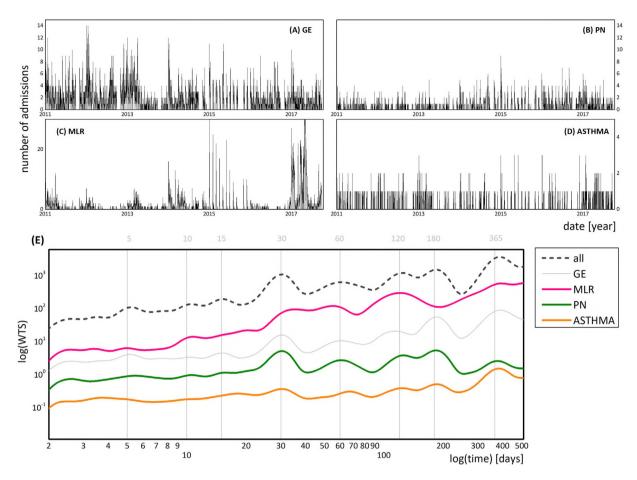
Fig. 3. Daily admission records for (A) GE, (B) pneumonia (PN), (C) malaria (MLR), and (D) asthma or asthmatic conditions with (E) WTS functions for these disorders, compared with WTS of all admissions data. In (E) vertical grey lines serve as visual guides for significant cycles.

at these scales. At these higher time scales, visible cycles in WTS appear at two, four and six months, followed by an annual peak. All the peaks in this record are statistically significant against the corresponding LTP noise as noise background, which was our choice for statistical significance testing, as shown in Supplemental material to this paper. The same overall significance was obtained for the white noise background of the stochastic AR (1) process used by (Torrence and Compo, 1998), while only cycles at 5 days, 30 days, 60 and 365 days are significant against the (Torrence and Compo, 1998) red noise AR(1) spectrum. This result was consistent for other records that we analysed.

In Fig. 3, we depict raw data for time series of GE, pneumonia, malaria and asthma admissions, together with their wavelet power spectra. The WTSs of these different diseases or conditions are presented in comparison with the WTS of all admissions data, displaying different slopes of WTS functions (which are given on log-log graphs in Fig. 3) with different cyclical consistency. This is especially prominent for pneumonia, malaria and asthma WTS functions that display prominence of higher order peaks (from 30 days onwards, particularly in the case of malaria) that could arise as effects of meteorological and environmental factors.
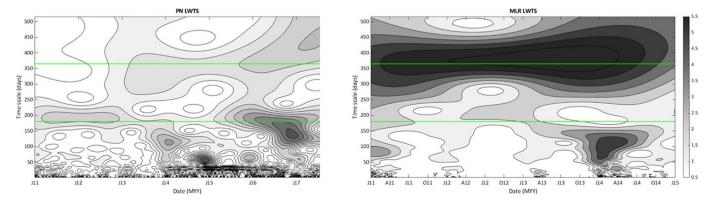

Fig. 4. LWTS for pneumonia (left) and malaria (right) admissions. Horizontal green lines at time scales (y-axis) values of 180 and 365 days are given to serve as visual guides. (For interpretation of the references to color in this figure legend, the reader is referred to the web version of this article.)

We further investigated pneumonia and malaria admissions data with respect to their potential meteorological or environmental drivers. In Fig. 4, we show LWTS of pneumonia and malaria admissions. We present pneumonia local wavelet spectra for the whole time period of 2011–2017, and malaria local wavelet spectra only for the period 2011–2015. Namely, in the case of the malaria data, because of a sudden increase in hospital admissions in 2015 and especially for the abrupt increase in cases in 2017 (see raw data in Fig. 3C) the LWTS and WTS
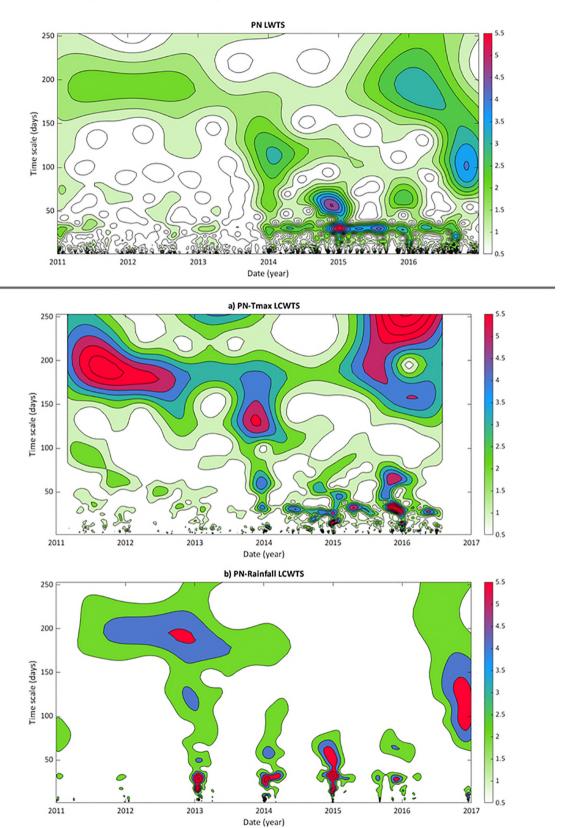

Fig. 5. LWTS of pneumonia admissions (top), with LCWTS of pneumonia admissions in comparison to Tmax records (a) and rainfall data (b). Panel (a) shows a visible 6-month cycle of pneumonia - Tmax coincidence that is present throughout the entire period of recording.

spectra of malaria display a prominent event over the time period from 2015 to mid-2017 (results not shown here). This is a methodological effect of the presence of extreme values in malaria record that appears due to the sensitivity of Morlet wavelets to significant singular events in data (Grossmann et al., 1987). It extends over all scales and significantly affects wavelet cross-spectra that compare malaria with other
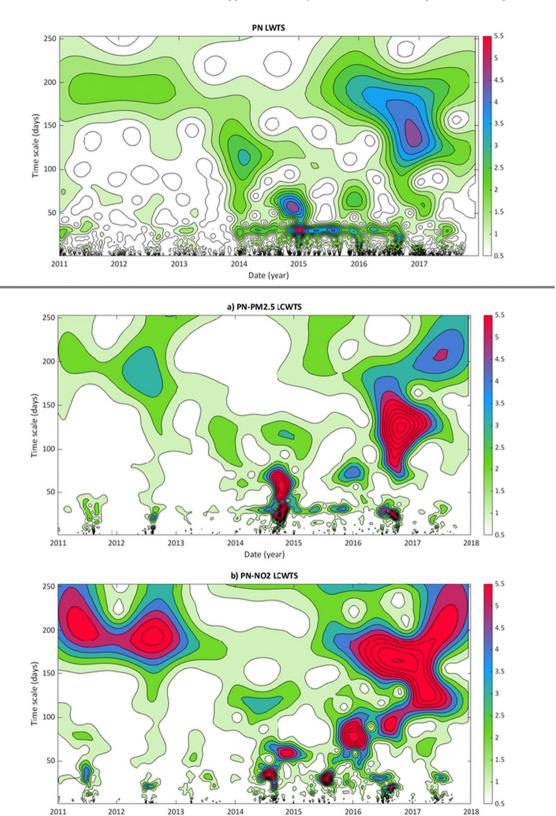

Fig. 6. LWTS of pneumonia admissions (top), with LCWTS of pneumonia admissions in comparison to PM$_{2.5}$ (a) and NO$_2$ data (b). Significant cross-correlations with both air quality variables are visible at lower scales, particularly for the period from 2014 onwards. In panel (a) a formation of a continuous 30-day cycle in cross-correlations of pneumonia with PM$_{2.5}$ is visible.

variables. Therefore, to avoid false detection of cross-correlations due to methodological limitations, we further limited the analysis that relates to malaria admissions to the time period 2011–2015.

It is visible from Fig. 4 that admissions for pneumonia and for malaria are statistically different variables. Admissions for pneumonia display complex structure, with appearance of events (admissions) distributed over the entire year (see structures that form at the onset of y-axis), and cycles (repetitions of events) forming visibly at short time scale values of less than 50 days, as well as at seasonal – 6-months and annual scales. In contrast, admissions for malaria are clearly events isolated to winter months, where they form at the start of y-axis and extend vertically to contribute to the dominant annual cycle and not so prominent 6-month cycle. In the case of admissions for malaria, and in the absence of physical causes or lower time scale structures from which those can originate, the appearance of a semi-annual cycle may present only as a sub-harmonic component of a dominant annual cycle.

In Figs. 5 and 6, we present results of the wavelet cross-correlation analysis of hospital admissions for pneumonia and the four physical variables: maximum temperature (Tmax), rainfall, $PM_{2.5}$ and NO_2 concentrations. The LCWTS given in Fig. 5 indicates that the Tmax may probably be a factor influencing pneumonia variability at larger scales. The temperature seasonality, due to the restriction of statistical significance of analysed scales here, visible only at a 6-months cycle in Fig. 5, is probably influencing seasonality in appearance of this disease. In addition, it is visible from Fig. 6 that the air quality variability probably significantly influences appearance of pneumonia at lower time scales. From Fig. 6, it appears that changes in concentrations of ambient $PM_{2.5}$ and NO_2 may influence prevalence of pneumonia on scales of up to 120 days, where patterns of pneumonia-air quality correlations follow in shape pneumonia LWTS patterns. This is particularly prominent in the period January 2014 to December 2017.

To investigate the co-dependence of admissions for pneumonia from air quality data at lower time scales, we narrowed the range of LCWT time scales (y-axis on LCWT graphs) to up to 64 days (Fig. 7). From Fig. 7, the structures forming cycles at 15 (and even 10) and 30 days are visible from LCWTSs of pneumonia in comparison to $PM_{2.5}$ and NO_2 concentrations. Considering that the appearance of pneumonia follows changes in air quality, the cycles at certain scales represent the delay of appearance of disease after physical events that may have been associated with them. In that respect, we added a global WTS of pneumonia records to Fig. 7 (graph on the right labelled (C)), where we marked cycles that could be attributed to physical variables that we investigated, along with other influences that we did not investigate. The cycles that are not marked are probably results of combinations of these and other effects that cannot be clearly differentiated by the analyses in this study.

In Figs. 8 and 9, results of the cross-correlation wavelet analysis of malaria records with meteorological and air quality data are presented and are analogous to results in Figs. 5 and 6. It is visible from Fig. 8 that the prominence of seasonal variations in malaria record translates into dominance of seasonal cycles in malaria versus Tmax cross-correlogram (Fig. 8a), and to an extent in cross-correlograms with air quality data in Fig. 9. Due to statistical significance, seasonality at annual time scales is outside of the range of our analysis, but we can presume that the annual seasonality is also present in malaria LCWTSs. The events on lower scales, when these appear, are probably connected to the combination of influences of temperature and rainfall. To inspect this, we calculated LCWTS of Tmax and rainfall (results are given in Supplemental material to this paper) – changes in those two meteorological variables indeed coincide almost exclusively during the rainy season, establishing conditions for combined effect on development of malaria.

Detailed analysis of Tmax and rainfall influence on malaria appearances for time scales of up to 128 days presented in Fig. 10 suggest
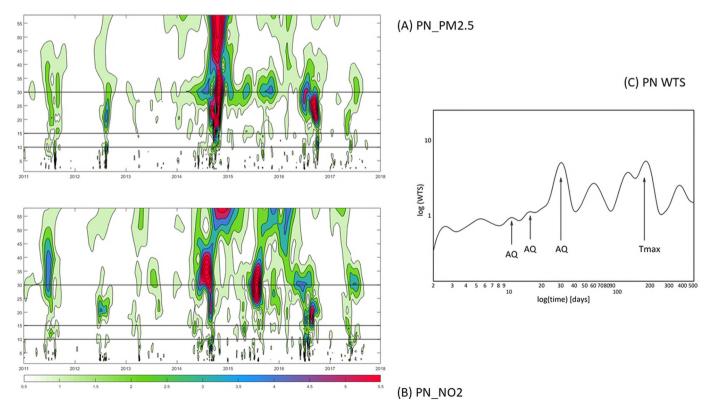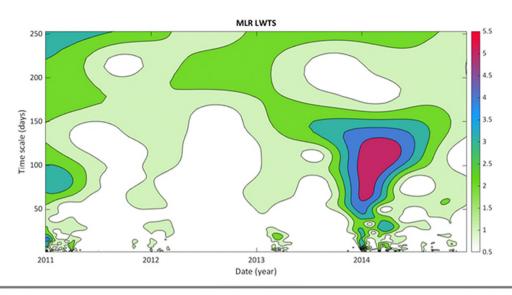

Fig. 7. Local wavelet cross spectra of pneumonia in comparison to $PM_{2.5}$ (A) and NO_2 (B) concentrations, for time scales on y-axes of up to 64 days. Horizontal lines at scales of 10, 15 and 30 days in (A) and (B) are given as visual guides. In the pneumonia WTS graph (C) cycles are marked that may result as effects of air quality or temperature. According to our results pneumonia may appear because of the change in air quality with 10-, 15- or 30-day delays.
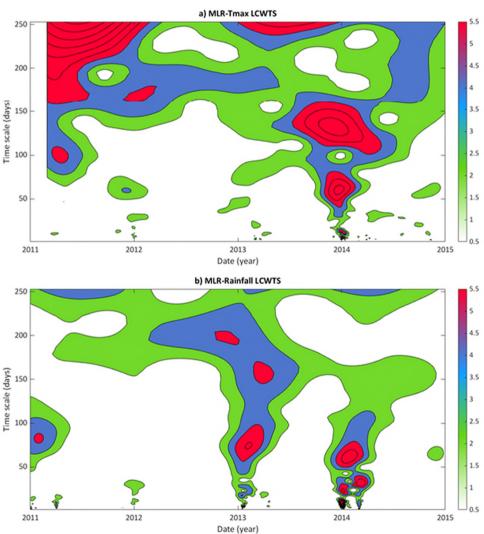
Fig. 8. LWTS of malaria admissions (top), with LCWTS of malaria admissions in comparison to Tmax records (a) and rainfall data (b). Figure shows probable combined influence of temperature and rainfall on formation of malaria LWTS structures on smaller (than 6 months) time scales.

that intermediate cycles visible in malaria global WTS at 30 and 60 days (Fig. 10 (C)) may be related to combined effects of temperature and rainfall. It is visible from LCWTSs of malaria versus Tmax and rainfall

data that these cycles are aperiodic, that is, they do not stretch across the entire time range of recording, but are isolated events caused by co-occurrence of heat and rainfall. They appear with changing strength
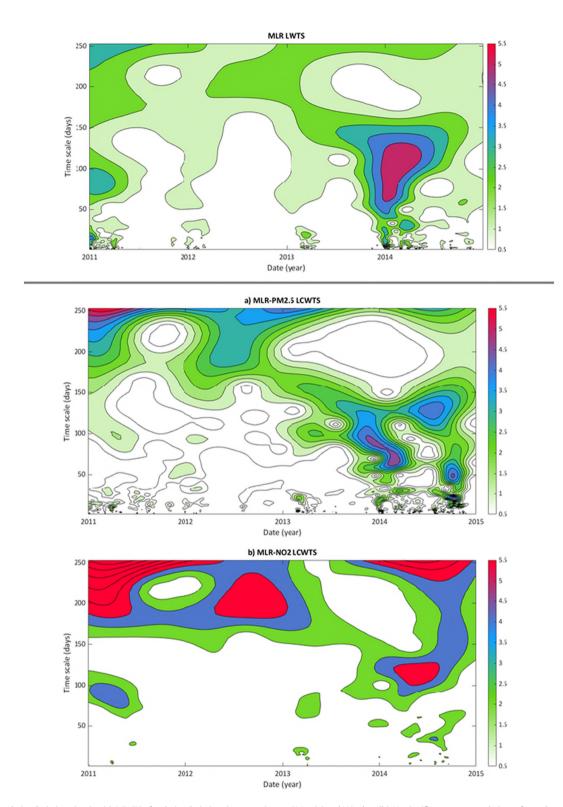
Fig. 9. LWTS of malaria admissions (top), with LCWTS of malaria admissions in comparison to $PM_{2.5}$ (a) and NO_2 data (b). No significant cross-correlations of prevalence of malaria with air quality variability are visible at lower time scales.

of cross-correlations with malaria prevalence during summer months of each year.

4. Discussion

We investigated the time series of daily hospital admissions for GE, asthma, pneumonia and malaria from two large public hospitals in Limpopo Province, in relation to time series of temperature, rainfall and air quality ground-based records or satellite data from the same geographical area. We were interested to disentangle physical, specifically, meteorological or environmental variables that might be associated with underlying temporal variations of disease prevalence measured through visits to hospitals. We used wavelet transform analysis and specifically local wavelet cross-correlation analysis for this purpose; to the best of our knowledge this is the first time these methods have been applied in weather/climate-health analyses.
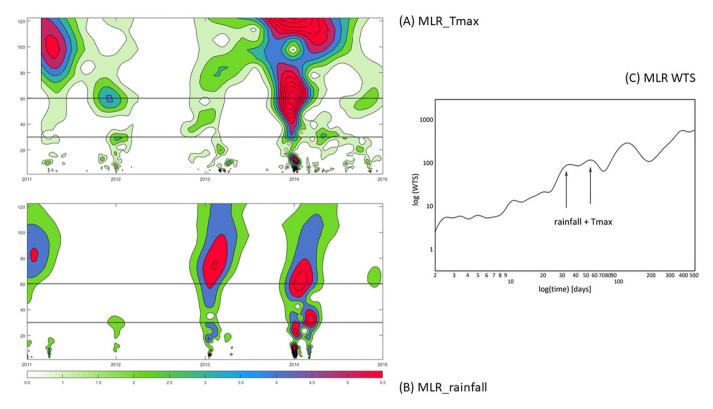
Fig. 10. Local wavelet cross spectra of MLR in comparison to Tmax (A) and rainfall (B) data, for time scales on y-axis of up to 128 days. MLR WTS is given in (C), in the same manner as in Fig. 6. Horizontal lines at time scales of 30 and 60 days in (A) and (B) serve as visual guides.

All our admission records have global wavelet power spectra (WTS) of the power-law type, indicating that they are outputs of complex sets of causes acting on different time scales. The 'all hospital admissions' dataset that we analysed showed the existence of cycles, or peaks in WTS that result from societal organization of daily life, on admission time scales of one to several working weeks or weeks.

We investigated WTS cycles that appeared on higher time scales in global admissions data in more detail for prevalence of pneumonia and malaria in our records. We used local wavelet cross-correlation spectra (LCWTs) to monitor coincidences in changes of meteorological (i.e., temperature and rainfall) and air quality (specifically concentrations of $PM_{2.5}$ and NO_2) variables with admissions to hospitals for these diseases. It is important to note here that, while in general no direct causal attribution is possible based on the power spectral or cross-power spectral analysis, the existence of auto- or cross-correlations between variables and established connections with triggered variable's (admissions, in this paper) significant WTS peaks are used to suggest a possible causal relationship. By using such an approach, we were able to provide new (other than already known seasonal variations) statistical estimates of time delays between the change of weather or air pollution and hospital admissions for pneumonia and malaria. In order to assess uncertainties related to provided associations between the hospital admissions and meteorological or air quality variables time series on a case-to-case basis, it is necessary to extend in the future our work in time series analysis to event-based event coincidence analysis (Donges et al., 2016).

The LCWTs for pneumonia data showed the existence of seasonality in the prevalence of pneumonia that could be 'connected' to changes in temperature. Even if admissions for pneumonia in our dataset occurred throughout all seasons, this result is in agreement with several other recent studies that investigated links between seasonal variations in pneumonia with changes in meteorological variables (Adegboye et al., 2020; Cilloniz et al., 2017; Tian et al., 2017). Those point to increased association of pneumonia hospitalization with low temperature; low

temperature effects are probably causing the annual seasonality of pneumonia in our dataset too. This pattern could be explained by findings that colder temperatures are associated with increased viral activity in regions of warmer climates (Lin et al., 2009). The influenza virus has been identified as a common cause of pneumonia and cold temperatures favour the spread of the virus (Lowen et al., 2007). Thus, the increased presence of circulating pathogens in the winter/colder months could result in the increased hospital admissions for pneumonia that were observed in our study. Furthermore, it has been suggested that exposure to cold air increases the incidence of respiratory infections by cooling the nasal epithelium thereby inhibiting respiratory defences against infection (Eccles, 2002). Another explanation for the increase in pneumonia hospital admissions with low temperatures, although controversial, is that cold stress alters the immune system and increases susceptibility to respiratory infections (Mäkinen et al., 2009). In addition, pneumonia admissions in this paper display a prominent semi-annual cycle that appears in pneumonia-Tmax LCWTSs in our sample too. The appearance of this cycle may be attributed to the impacts of the increase of rainfall in wet seasons on pneumonia (Adegboye et al., 2020; Xu et al., 2014) that, by way of high temperature-rainfall coincidence, presents in pneumonia-Tmax LCWTSs as well. High rainfall and low temperatures could also lead to increased crowding of people indoors thus increasing contact between people and increasing the distribution of pathogens (Chowdhury et al., 2018). Rain-wetting was also found to be associated significantly with the development of influenza pneumonia (Singh et al., 2014). Furthermore, heavy rainfall can result in water intrusion into buildings and populations living in damp, indoor environments have been shown to experience increased prevalence of respiratory illnesses (CDC, 2020). Overall, the factors influencing seasonal appearance of pneumonia with the change of temperature and rainfall could be caused by the human activity, seasonal variability in human immune system function, or effects of cold air on respiratory defences against infections (Fares, 2013; Eccles, 2002; Adegboye et al., 2020). Our results have not clearly indicated lag times between changes

in meteorological variables and seasonal prevalence of pneumonia. Adegboye et al. (2020) used time-varying distributed lag nonlinear model for the purpose and found time lags of 0–6 weeks for effects of low temperature and 0–8 weeks for effects of rainfall on hospitalization for pneumonia in North Australia.

Our LCWTS analysis additionally showed probable 'preconditioning' (Zscheischler et al., 2020) of pneumonia by changes in air quality. In a preconditioned event, a hazard such as disease can develop only because of a pre-existing climate-driven health condition (Zscheischler et al., 2020). In our data, the effects of air quality on pneumonia appeared on time scales of 10 to 15 and 30 days. This gave a period (also called a lag or delay) of 10–15 days between the change in air quality and development of pneumonia or pneumonia-related diseases, with the cycle at 30 days that can be a multiple of this period or an independent air quality-related delay. The relation of change in air quality with development of respiratory diseases is well documented (Schwartz et al., 1991; Gruzieva et al., 2013; Wu et al., 2020). Previous research has shown that long-term exposure to pollutants such as $PM_{2.5}$ or NO_2 reduces lung function (Kwon et al., 2020; Adam et al., 2015; Chen et al., 2019) and can cause persistent inflammatory response that increases the risk of infection by viruses that target the respiratory tract (Croft et al., 2019; Domingo and Rovira, 2020). Our study adds to this body of knowledge by both confirming the causal relation between air quality and prevalence of respiratory diseases, and by additionally providing a statistical estimate of the time delay between the change in air quality and hospital admissions for pneumonia specifically.

We found seasonal correlation in hospital admissions for malaria with temperature variations. Local wavelet cross-correlation analysis additionally showed that malaria is probably a multivariate event (Zscheischler et al., 2020) caused by co-occurrence of specific temperature conditions (namely heat) and rainfall. Aside from a visible seasonality in malaria prevalence, our LCWTS data showed that it probably follows the co-occurrence of high temperature and rainfall after a 30-day interval. This association was most noticeable during the summer months of November, December, January, and February which are characterized by high temperature and rainfall. This finding is corroborated by previous studies conducted in Limpopo province that have found malaria prevalence peak during these months (Gerritsen et al., 2008; Ikeda et al., 2017). High temperatures increase malaria transmission because warm conditions promote malaria parasite development and growth and increase the survival rate (Craig et al., 1999). Also, since mosquitoes develop faster as temperature increases, they feed at shorter intervals because blood meals are more rapidly digested thus increasing risk of malaria transmission (Grover-Kopec et al., 2006; Hay et al., 2000; Musa et al., 2012).

In South Africa, variations in air quality can be caused by anthropogenic aerosols, such as biomass burning, vehicle and industry emissions, as well as population, geography, climate and economy (Kumar et al., 2014). Although a seasonality of these changes exists for the winter season, there also exist multiple factors that can cause air quality change during the entire year that therefore pose challenges when planning preventive public health interventions. Characterization and quantification of physical causes and connected delay (disease development) times for respiratory diseases of the kind presented in this study may be a way forward to assist such efforts.

Our study furthermore provides a measure of time needed for all the conditions for malaria to develop after the onset of its meteorological driver. It thus links observed seasonality in prevalence of malaria with climate change and its impacts on multivariate events caused by co-occurrence of heat and humidity (Raymond et al., 2020).

A few limitations were identified during this study. Firstly, all the hospital records were handwritten and posed numerous challenges such as faded ink and handwriting being illegible, daily use of books leading to torn pages, errors in recording (for example: a male patient captured in a female ward) and missing data (for example: date of admission and patient age). In this way a large part of the collected dataset was unusable for the statistical analysis. This in turn constrained our analysis to time scales of up to approximately 250 days and prevented our insight into annual and multiannual cycles of hospital admissions data. It specifically prompted us to exclude asthma records from detailed statistical analysis. In our dataset, admissions for asthma records showed prominent seasonal variations for which we did not have enough data points to conduct statistically significant analysis. Additionally, we decided to exclude GE records from detailed WT analysis due to inability to differentiate between various gastrointestinal ailments. Therefore, we were not able to investigate climate or environmental drivers of, for example, diarrhoeal disease, which is a major contributor to the burden of infectious disease among young children in sub-Saharan Africa (WHO, 2018). This limitation could be mitigated in the future by digitalization of hospital records that may offer possibilities to flag diarrhoeal diseases and thus include it in hospital statistics.

With respect to weather data, due to the lack of ground-based observations of air quality in the Giyani region, reanalysis data were used. Although the current CAMS model has smaller biases O_3, CO and NO_2 compared with observations than previous versions there are still uncertainties due to the inherent properties of numerical models, relating to observational datasets, parameterizations, and spatial and temporal resolution. It is possible that the data pre-processing averages out details of statistical behaviour of air quality variables in time (Bunde and Lennartz, 2012) and over space (Blesić et al., 2019). This leads to lack of complexity in their wavelet cross-correlations with disease prevalence too. In that respect it is preferable to use data with better spatial resolution whenever it is possible to avoid methodological uncertainty and obtain more accurate or even novel results (Blesić et al., 2019).

5. Conclusions

Causal relationships identified in this study – i.e., preconditioning and joint occurrence – between meteorological or air quality variables and health outcomes, together with specified time delay parameters between the onset of a driver and development of a disease, may be of use as parameter inputs to and non-trivial realistic tests for the predictive models and early warning systems of exposure and health impacts of climate change. They can additionally serve as a data-led understanding to inform relevant local actors and help facilitate novel adaptation measures in public health systems.

CRediT authorship contribution statement

Thandi Kapwata: Methodology, Formal analysis, Writing – original draft, Writing – review & editing. **Caradee Y. Wright:** Conceptualization, Project administration, Writing – original draft, Writing – review & editing. **David Jean du Preez:** Writing – original draft, Writing – review & editing. **Zamantimande Kunene:** Writing – review & editing. **Angela Mathee:** Funding acquisition, Writing – review & editing. **Takayoshi Ikeda:** Writing – review & editing. **Willem Landman:** Writing – review & editing. **Rajendra Maharaj:** Writing – review & editing. **Neville Sweijd:** Writing – review & editing. **Noboru Minakawa:** Writing – review & editing. **Suzana Blesic:** Conceptualization, Methodology, Formal analysis, Writing – original draft, Writing – review & editing.

Declaration of competing interest

The authors declare that they have no conflicts of interest.

References

Adam, M., Schikowski, T., Carsin, A.E., Cai, Y., Jacquemin, B., Sanchez, M., et al., 2015. Adult lung function and long-term air pollution exposure. ESCAPE: a multicentre cohort study and meta-analysis. Eur. Respir. J. 45, 38–50 PMID: 25193994. https://doi.org/10.1183/09031936.00130014.

Addison, P.S., 2002. The Illustrated Wavelet Transform Handbook: Introductory Theory and Applications in Science, Engineering, Medicine and Finance. 1st edition. Napier University, Edinburgh, UK https://www.routledge.com/The-Illustrated-Wavelet-Transform-Handbook-Introductory-Theory-and-Applications/Addison/p/book/9780367574000.

Addison, P.S., 2018. Introduction to redundancy rules: the continuous wavelet transform comes of age. Philos. Trans. R. Soc. A Math. Phys. Eng. Sci. https://doi.org/10.1098/rsta.2017.0258.

Adegboye, O.A., McBryde, E.S., Eisen, D.P., 2020. Epidemiological analysis of association between lagged meteorological variables and pneumonia in wet-dry tropical North Australia, 2006–2016. J. Expos. Sci. Environ. Epidemiol. 30 (3), 448–458.

Aguiar-Conraria, L., Soares, M.J., 2014. The continuous wavelet transform: moving beyond uni- and bivariate analysis. J. Econ. Surv. 28 (2), 344–375. https://doi.org/10.1111/joes.12012.

Akompab, D.A., Bi, P., Williams, S., Grant, J., Walker, I.A., Augoustinos, M., 2013. Awareness of and attitudes towards heat waves within the context of climate change among a cohort of residents in Adelaide, Australia. Int. J. Environ. Res. Publ. Health 10, 1–17 PMID: 23343978. https://doi.org/10.3390/ijerph10010001.

Astaf'eva, N.M., 1996. Wavelet analysis: basic theory and some applications. Physics-Uspekhi 39, 1085. https://doi.org/10.1070/pu1996v039n11abeh000177.

Blešić, S., Zanchettine, D., Rubino, A., 2019. Heterogeneity of scaling of the observed global temperature data. J. Clim. 32 (2), 349–367. https://doi.org/10.1175/JCLI-D-17-0823.1.

Bohnenstengel, S., Belcher, S., Aiken, A., Allan, J., Allen, G., Bacak, A., et al., 2015. Meteorology, air quality, and health in London: the ClearfLo project. Bull. Am. Met. Soc. 96, 779–804. https://doi.org/10.1175/BAMS-D-12-00245.1.

Bunde, A., Lennartz, S., 2012. Long-term correlations in earth sciences. Acta Geophys. 60, 562–588.

CDC, 2020. Centers for Disease Control and Prevention (CDC): Climate Effects on Health - Precipitation Extremes: Heavy Rainfall, Flooding, and Droughts. Available at. https://www.cdc.gov/climateandhealth/effects/precipitation_extremes.htm.

Chen, C.-H., Wu, C.-D., Chiang, H.-C., Chu, D., Lee, K.-Y., Lin, W.-Y., et al., 2019. The effects of fine and coarse particulate matter on lung function among the elderly. Sci. Rep. 9, 1–8 PMID: 31616001. https://doi.org/10.1038/s41598-019-51307-5.

Chowdhury, F.R., et al., 2018. The association between temperature, rainfall and humidity with common climate-sensitive infectious diseases in Bangladesh. PLoS One 13 (6), e0199579.

Christiansen, T.B., Lauritsen, J.M., 2010. EpiData—Comprehensive Data Management and Basic Statistical Analysis System. EpiData Association, Odense, Denmark http://www.epidata.dk.

Christophe, Y., Bennouna, Y., Schulz, M., Eskes, H.J., Basart, S., Benedictow, A.M., et al., 2017. Validation report of the CAMS global reanalysis of aerosols and reactive gases, years 2003–2018. http://atmosphere.copernicus.eu/.

Cilloniz, C., Ewig, S., Gabarrus, A., Ferrer, M., Puig de la Bella Casa, J., Mensa, J., Torres, A., 2017. Seasonality of pathogens causing community-acquired pneumonia. Respirology (Carlton, Vic.) 22 (4), 778–785.

Climate Dialogue, 2014. Extended Summary of the Climate Dialogue on Long Term Persistence. https://www.mwenb.nl/wp-content/uploads/2014/04/Climatedialogue.org-extended-summary-long-term-persistence.pdf.

CPC, 2001. Climate Prediction Center (CPC) Rainfall Estimator (RFE) for Africa. https://data.noaa.gov/dataset/dataset/climate-prediction-center-cpc-rainfall-estimator-rfe-for-africa.

Craig, M.H., Snow, R.W., le Sueur, D., 1999. A climate-based distribution model of malaria transmission in Sub-Saharan Africa. Parasitol. Today 15, 105–111.

Croft, D.P., Zhang, W., Lin, S., Thurston, S.W., Hopke, P.K., Masiol, M., et al., 2019. The association between respiratory infection and air pollution in the setting of air quality policy and economic change. Ann. Am. Thor. Soc. 16, 321–330 PMID: 30398895. https://doi.org/10.1513/annalsats.201810-691oc.

Dai, A., 2011. Drought under global warming: a review. WIREs Clim. Change 2, 45–65. https://doi.org/10.1002/wcc.81.

Domingo, J.L., Rovira, J., 2020. Effects of air pollutants on the transmission and severity of respiratory viral infections. Environ. Res. 187, 109650 PMID: 32416357. https://doi.org/10.1016/j.env.res.2020.109650.

Donges, J.F., Schleussner, C.F., Siegmund, J.F., Donner, R.V., 2016. Event coincidence analysis for quantifying statistical interrelationships between event time series. Eur. Phys. J. Spec. Top. 225 (3), 471–487.

Ebi, K., Mearns, L., Nyenzi, B., 2003. Weather and climate: changing human exposures. Climate Change and Health: Risks and Responses. World Health Organization, Geneva https://www.who.int/globalchange/publications/climatechangechap2.pdf.

Eccles, R., 2002. An explanation for the seasonality of acute upper respiratory tract viral infections. Acta Otolaryngol. 122, 183–191.

ECMWF, 2021. CAMS: reanalysis data documentation. https://confluence.ecmwf.int/display/CKB/CAMS%3A+Reanalysis+data+documentation.

Fares, A., 2013. Factors influencing the seasonal patterns of infectious diseases. Int. J. Prev. Med. 4, 128.

Farge, M., 1992. Wavelet transforms and their applications to turbulence. Annu. Rev. Fluid Mech. 24 (1), 395–458.

Fouillet, A., Rey, G., Laurent, F., Pavillon, G., Bellec, S., Guihenneuc-Jouyaux, C., et al., 2006. Excess mortality related to the August 2003 heat wave in France. Int. Arch. Occup. Environ. Health. 80, 16–24 PMID: 16523319. https://doi.org/10.1007/s00420-006-0089-4.

Franchini, M., Mannucci, P.M., 2015. Impact on human health of climate changes. Eur. J. Int. Med. 26, 1–5 PMID: 25582074. https://doi.org/10.1016/j.ejim.2014.12.008.

Frick, P., Beck, R., Berkhuijsen, E.M., Patrickeyev, I.T., 2001. Scaling and correlation analysis of galactic images. Mon. Not. R. Astron. Soc. 327 (4), 1145–1157. https://doi.org/10.1045/j.1365-8711.2001.04812.x.

Gerritsen, A.A., Kruger, P., Van Der Loeff, M.F.S., Grobusch, M.P., 2008. Malaria incidence in Limpopo Province, South Africa, 1998–2007. Malar. J. 7, 162. https://doi.org/10.1186/1475-2875-7-162.

Godsmark, C.N., Irlam, J., van der Merwe, F., New, M., Rother, H.-A., 2019. Priority focus areas for a sub-national response to climate change and health: a South African provincial case study. Environ. Int. 122, 31–51 PMID: 30573189. https://doi.org/10.1016/j.envint.2018.11.035.

Goupillaud, P., Grossmann, A., Morlet, J., 1984. Cycle-octave and related transforms in seismic signal analysis. Geoexploration 23 (1), 85–102. https://doi.org/10.1016/0016-7142(84)90025-5.

Grossmann, A., Morlet, J., 1984. Decomposition of hardy functions into square Integrable wavelets of constant shape. SIAM J. Math. Anal. 15 (4), 723–736. https://doi.org/10.1137/0515056.

Grossmann, A., Holschneider, M., Kronland-Matinet, R., Morlet, J., 1987. Detection of abrupt changes in sound signals with the help of the wavelet transform, inverse problems: an interdisciplinary study. Adv. Electron. Electron Phys. 19, 298–306.

Grover-Kopec, E., Blumenthal, M.B., Ceccato, P., Dinku, T., Omumbo, J., Connor, S., 2006. Web-based climate information resources for malaria control in Africa. Malar. J. 5, 38.

Gruzieva, O., Bergström, A., Hulchiy, O., Kull, I., Lind, T., Melén, E., et al., 2013. Exposure to air pollution from traffic and childhood asthma until 12 years of age. Epidemiology 24 (1), 54–61 PMID: 23222555. https://doi.org/10.1097/EDE.0b013e18276c1ea.

Hales, S., Edwards, S., Kovats, R., 2003. Impacts on Health of Climate Extremes, Climate Change and Human Health: Risks and Responses. , pp. 79–102. https://www.who.int/globalchange/publications/climatechangechap5.pdf.

Hanna, A.F., Yeatts, K.B., Xiu, A., Zhu, Z., Smith, R.L., Davis, N.N., et al., 2011. Associations between ozone and morbidity using the spatial synoptic classification system. Environ. Health 10, 49 PMID: 21609456. https://doi.org/10.1186/1476-069X-10-49.

Hay, S.I., Omumbo, J.A., Craig, M.H., Snow, R.W., 2000. Earth observation, geographic information systems and Plasmodium falciparum malaria in sub-Saharan Africa. Adv. Parasitol. 47, 173–215.

Hirabayashi, Y., Mahendran, R., Koirala, S., Konoshima, L., Yamazaki, D., Watanabe, S., et al., 2013. Global flood risk under climate change. Nat. Clim. Change 3, 816–821. https://doi.org/10.1038/nclimate1911.

Ikeda, T., Behera, S.K., Morioka, Y., Minakawa, N., Hashizume, M., Tsuzuki, A., et al., 2017. Seasonally lagged effects of climatic factors on malaria incidence in South Africa. Sci. Rep. 7, 1–9. https://doi.org/10.1038/s41598-017-02680-6.

Ikeda, T., Kapwata, T., Behera, S.K., Minakawa, N., Hashizume, M., Sweijd, N., et al., 2019. Climatic factors in relation to diarrhoea hospital admissions in rural Limpopo, South Africa. Atmosphere 10, 522. https://doi.org/10.3390/atmos10090522.

Inness, A., Ades, M., Agustí-Panareda, A., Barré, J., Benedictow, A., Blechschmidt, A.-M., et al., 2019. The CAMS reanalysis of atmospheric composition. Atmos. Chem. Phys. 19, 3515–3556. https://doi.org/10.5194/acp-19-3515-2019.

Jhun, I., Coull, B.A., Schwartz, J., Hubbell, B., Koutrakis, P., 2015. The impact of weather changes on air quality and health in the United States in 1994–2012. Environ. Res. Lett. 10, 084009. https://iopscience.iop.org/article/10.1088/1748-9326/10/8/084009.

Kinney, P.L., 2008. Climate change, air quality, and human health. Am. J. Prev. Med. 35, 459–467 PMID: 18929972. https://doi.org/10.1016/j.amepre.2008.08.025.

Koscielny-Bunde, E., Kantelhardt, J.W., Braun, P., Bunde, A., Havlin, S., 2006. Long-term persistence and multifractality of river runoff records: detrended fluctuation studies. J. Hydrol. 322 (1–4), 120–137. https://doi.org/10.1016/j.jhydrol.2005.03.004.

Kumar, K.R., Sivakumar, V., Yin, Y., Reddy, R., Kang, N., Diao, Y., et al., 2014. Long-term (2003–2013) climatological trends and variations in aerosol optical parameters retrieved from MODIS over three stations in South Africa. Atmos. Environ. 95, 400–408. https://doi.org/10.1016/j.scitotenv.2013.04.095.

Kwon, S.O., Hong, S.H., Han, Y.-J., Bak, S.H., Kim, J., Lee, M.K., et al., 2020. Long-term exposure to PM$_{10}$ and NO$_2$ in relation to lung function and imaging phenotypes in a COPD cohort. Respir. Res. 21, 1–11 PMID: 32967681. https://doi.org/10.1186/s12931-020-01514-w.

Lancaster, G., Iatsenko, D., Pidde, A., Ticcinelli, V., Stefanovska, A., 2018. Surrogate data for hypothesis testing of physical systems. Phys. Rep. 748, 1–60. https://doi.org/10.1016/j.physrep.2018.06.001.

Lin, H.-C., et al., 2009. Seasonality of pneumonia admissions and its association with climate: an eight-year nationwide population-based study. Chronobiol. Int. 26 (8), 1647–1659.

Lokotola, C.L., Wright, C.Y., Wichmann, J., 2020. Temperature as a modifier of the effects of air pollution on cardiovascular disease hospital admissions in Cape Town, South Africa. Environ. Sci. Pollut. Res. Int. 27 (14), 16677–16685 PMID: 32133609. https://doi.org/10.1007/s11356-020-07938-7.

Lowen, A.C., et al., 2007. Influenza virus transmission is dependent on relative humidity and temperature. PLoS Pathog. 3 (10), e151.

Mäkinen, T.M., et al., 2009. Cold temperature and low humidity are associated with increased occurrence of respiratory tract infections. Respir. Med. 103 (3), 456–462.

Morlet, J., 1983. Sampling theory and wave propagation. Issues in Acoustic Signal/Image Processing and Recognition. Springer, Berlin Heidelberg, pp. 233–261 https://doi.org/10.1007/978-3-642-82002-1_12.

Musa, M.I., Shohaimi, S., Hashim, N.R., Krishnarajah, I., 2012. A climate distribution model of malaria transmission in Sudan. Geospat. Health 7 (1), 27–36.

Nitschke, M., Tucker, G.R., Hansen, A.L., Williams, S., Zhang, Y., Bi, P., 2011. Impact of two recent extreme heat episodes on morbidity and mortality in Adelaide, South Australia: a case-series analysis. Environ. Health 10, 42 PMID: 21592410. https://doi.org/10.1186/1476-069X-10-42.

Papanastasiou, D., Melas, D., Kambezidis, H., 2015. Air quality and thermal comfort levels under extreme hot weather. Atmos. Res. 152, 4–13. https://doi.org/10.1016/j.atmosres.2014.06.002.

Perrier, V., Philipovitch, T., Basdevant, C., 1995. Wavelet spectra compared to Fourier spectra. J. Math. Phys. 36 (3), 1506–1519. https://doi.org/10.1063/1.531340.

Raymond, C., Horton, R.M., Zscheischler, J., Martius, O., Aghakouchak, A., Balch, J., et al., 2020. Understanding and managing connected extreme events. Nat. Clim. Chang. 10, 611–621. https://doi.org/10.1038/s41558-020-0790-4.

Rhif, M., Ben Abbes, A., Farah, I.R., Martínez, B., Sang, Y., 2019. Wavelet transform application for/in non-stationary time-series analysis: a review. Appl. Sci. 9 (7), 1345.

Rodríguez-Murillo, J.C., Filella, M., 2020. Significance and causality in continuous wavelet and wavelet coherence spectra applied to hydrological time series. Hydrology 7 (4), 82.

Rust, H.W., Mestre, O., Venema, V.K., 2008. Fewer jumps, less memory: homogenized temperature records and long memory. J. Geophys. Res. 113, D19110. https://doi.org/10.1029/2008JD009919.

Schwartz, J., Spix, C., Wichmann, H.E., Malin, E., 1991. Air pollution and acute respiratory illness in five German communities. Environ. Res. 56 (1), 1–14 PMID: 1915187. https://doi.org/10.1016/s0013-9351(05)80104-5.

Scovronick, N., Sera, F., Acquaotta, F., Garzena, D., Fratianni, S., Wright, C.Y., et al., 2018. The association between ambient temperature and mortality in South Africa: a time-series analysis. Environ. Res. 161, 229–235 PMID: 29161655. https://doi.org/10.1016/j.envres.2017.11.001.

Seneviratne, S., Nicholls, N., Easterling, D., Goodess, C., Kanae, S., Kossin, J., et al., 2012. Changes in climate extremes and their impacts on the natural physical environment. Managing the Risks of Extreme Events and Disasters to Advance Climate Change Adaptation. A Special Report of Working Groups I and II of the Intergovernmental Panel on Climate Change (IPCC). Cambridge University Press, Cambridge, UK, and New York, NY, USA , pp. 109–230. https://www.ipcc.ch/site/assets/uploads/2018/03/SREX-Chap3_FINAL-1.pdf.

Singh, V., et al., 2014. Clinical profile of pneumonia and its association with rain wetting in patients admitted at a tertiary care institute during pandemic of influenza A (H1N1) pdm09 virus infection. Indian J. Chest Dis. Allied Sci. 56 (1), 21–26.

Singh, P., Shiv Dutt, J., Kumar, P.R., Kaushik, S., 2017. The Fourier decomposition method for nonlinear and non-stationary time series analysis. Proc. R. Soc. A 473, 20160871 PMID: 28413352. https://doi.org/10.1098/rspa.2016.0871.

Stratimirović, D., Milošević, S., Blesić, S., Ljubisavljević, M., 2001. Wavelet analysis of discharge dynamics of fusimotor neurons. Phys. A Stat. Mech. Appl. 291 (1–4), 13–23.

Stratimirović, D., Milošević, S., Blesić, S., Ljubisavljević, M., 2007. Wavelet transform analysis of time series generated by the stimulated neuronal activity. Phys. A Stat. Mech. Appl. 374 (2), 699–706. https://doi.org/10.1016/j.physa.2006.08.075.

Stratimirović, D., Sarvan, D., Miljković, V., Blesić, S., 2018. Analysis of cyclical behavior in time series of stock market returns. Commun. Nonlinear Sci. Numer. Simul. 54, 21–33. https://doi.org/10.1016/j.cnsns.2017.05.009.

Sun, X., Sun, Q., Yang, M., Zhou, X., Li, X., Yu, A., et al., 2014. Effects of temperature and heat waves on emergency department visits and emergency ambulance dispatches in Pudong New Area, China: a time series analysis. Environ. Health 13, 76 PMID: 25273545. https://doi.org/10.1186/1476-069X-13-76.

Thomson, M.C., Rabie, T.S., Shumake-Guillemot, J., McDermott, J., James, W., Wannous, C., 2019. Health priorities in a changing climate. In Climate Information for public health action. In: Thomson, M.C., Mason, S.J. (Eds.), Routlegde Published, Abingdon, Oxonl New York, NY. ISBN: 9781315115603.

Tian, D.D., Jiang, R., Chen, X.J., Ye, Q., 2017. Meteorological factors on the incidence of MP and RSV pneumonia in children. PLoS One 12 (3), e0173409.

Torrence, C., Compo, G.P., 1998. A practical guide to wavelet analysis. Bull. Am. Meteorol. Soc. 79 (1), 61–78. https://doi.org/10.1175/1520-0477(1998)079<0061:APGTWA>2.0.CO;2.

Vanos, J.K., Hebbern, C., Cakmak, S., 2014. Risk assessment for cardiovascular and respiratory mortality due to air pollution and synoptic meteorology in 10 Canadian cities. Environ. Pollut. 185, 322–332 PMID: 24355413. https://doi.org/10.1016/j.envpol.2013.11.007.

Vanos, J., Cakmak, S., Kalkstein, L., Yagouti, A., 2015. Association of weather and air pollution interactions on daily mortality in 12 Canadian cities. Air Quality Atmos. Health 8, 307–320. https://doi.org/10.1007/s11869-014-0266-7.

Wichmann, J., 2017. Heat effects of ambient apparent temperature on all-cause mortality in Cape Town, Durban and Johannesburg, South Africa: 2006–2010. Sci. Total Environ. 587, 266–272 PMID: 28242220. https://doi.org/10.1016/j.scitotenv.2017.02.135.

WMO, 2013. The Global Climate 2001–2010: A Decade of Climate Extremes, Summary Report. World Meteorological Association, Geneva, Switzerland https://library.wmo.int/index.php?lvl=notice_display&id=15112.

World Health Organization, 2006. Air quality guidelines: global update 2005: particulate matter, ozone, nitrogen dioxide, and sulfur dioxide. https://www.euro.who.int/en/health-topics/environment-and-health/air-quality/publications/pre2009/air-quality-guidelines.-global-update-2005.-particulate-matter,-ozone,-nitrogen-dioxide-and-sulfur-dioxide.

World Health Organization, 2018. World Malaria Report 2018. https://www.who.int/malaria/publications/world_malaria_report/en/.

Wu, X., Nethery, R.C., Sabath, B.M., Braun, D., Dominici, F., 2020. Exposure to air pollution and COVID-19 mortality in the United States: a nationwide cross-sectional study. medRxiv: the preprint server for health sciences https://doi.org/10.1101/2020.04.05.20054502 2020.04.05.20054502.

Xu, Z., Liu, Y., Ma, Z., Li, S/., Hu, W., Tong, S., 2014. Impact of temperature on childhood pneumonia estimated from satellite remote sensing. Environ. Res. 132, 334–341.

Ziervogel, G., New, M., Archer Van Garderen, E., Midgley, G., Taylor, A., Hamann, R., et al., 2014. Climate change impacts and adaptation in South Africa. WIREs Clim. Change 5, 605–620. https://doi.org/10.1002/wcc.295.

Zscheischler, J., Martius, O., Westra, S., Bevacqua, E., Raymond, C., Horton, R.M., et al., 2020. A typology of compound weather and climate events. Nat. Rev. Earth Environ. 1 (7), 333–347. https://doi.org/10.1038/s43017-020-0060-z.